The High Resolution Far Infrared Spectrum of Diacetylene, Obtained with a Michelson Interferometer *

F. Winther

Abt. Chemische Physik, Institut für Physikalische Chemie der Universität Kiel

(Z. Naturforsch. **28 a**, 1179–1185 [1973]; received 7 March 1973)

A commercial interferometer has been modified for high resolution gas phase work by addition of a variable temperature cell of 3 m path length. The data reduction method is described, and examples of the performance are given. Two rotation-vibration bands of diacetylene, ν_9 and $\nu_7-\nu_9$, have been analyzed to yield $\nu_9=220.139(5)$, $\nu_7=482.13(1)$, and $B_0=0.14649(7)$ cm^{-1}.

Introduction

During the last decade a large number of interferometers have been built for different regions of the infrared and several are available commercially. The purpose of this investigation was to develop from a commercial Michelson interferometer a configuration suitable for high resolution gas phase work in the range $400-50$ cm^{-1}, and to test the performance near the resolution limit.

Diacetylene with $2B \approx 0.29$ cm^{-1} was one of the largest linear molecules whose band structure the interferometer was expected to resolve. Rather inadvertently the ν_9 and $\nu_7-\nu_9$ bands of this molecule proved to be a severe resolution test because of several overlapping hot bands, persistent even at low temperature. This emphasizes that cooling of the gas cell is essential for obtaining resolved spectra of molecules with one or more low frequency levels. The spectra were obtained from an off-line Fourier transformation because of the large number of sampling points to be used for simultaneous recording of several hundred wavenumbers. During the development it turned out that the instrument attained a resolution of 0.08 cm^{-1} at 200 cm^{-1} and at least 0.3 cm^{-1} near the present high frequency limit of 670 cm^{-1} (polyethylene absorption). Work is going on to improve the high frequency performance further.

1. The Interferometer and Data Reduction

A Michelson interferometer for the far infrared region (Beckman-RIIC FS-720) has been equipped with a 3 m absorption cell as shown in Figure 1.

Reprint requests to Dr. F. Winther, Institut für Physikal. Chemie der Universität Kiel, Abt. Chemische Physik, *D-2300 Kiel*, Olshausenstraße 40–60.

The cell is stainless steel tube of 71 mm internal diameter with interchangeable windows, in the present configuration consisting of 2 mm polyethylene. Apart from two short sections near the windows, which are kept at room temperature, the cell is fitted with a system of cooling tubes allowing temperatures between ambient and -90 °C to be obtained by means of a cryostat. Contrary to cells of the light pipe [1] or White [2] type the loss of radiation in the present cell arises mainly from the windows. For the spectral range $400-50$ cm^{-1} the attenuation is about 0.1 dB. A disadvantage is the large volume, because of the parallel light beam at full aperture through the cell.

The rest of the optical system of the interferometer was left unchanged, except that the condensing lens in front of the Golay detector was replaced by black (40 μ) polyethylene foil. Generally two different poly(ethyleneterephtalate) ** beamsplitters have been used, 6 μ for the range $400-50$ cm^{-1} and 3.5 μ for the range $650-150$ cm^{-1}. Depending upon the frequency interval of interest, additional alkali halide high pass filters have been inserted in front of the detector. A source aperture of 10 mm diameter has been used throughout.

The maximum travelling distance of the moving mirror is ± 5 cm (optical path length ± 10 cm), giving a minimum half linewidth of 0.08 cm^{-1} without apodization of the spectra [3]. This figure equals the resolution in Figure 3. Figure 2 shows some other examples of the performance of the interferometer. To obtain the highest resolution between 400 and 100 cm^{-1} an (optical) sampling distance of 8 μ was used, giving a one-sided interferogram of 12 500 points. This means an oversampling factor of approximately 2. To improve the signal to noise ratio further, several spectra were averaged after the

* Preliminary results from this paper have been reported on the Coll. on High. Res. Molecular Spectry., Dijon 1971 and on the 2' Int. Sem. on High Res. IR Spectry., Prague 1972.

** Mylar®, Hostaphan®.

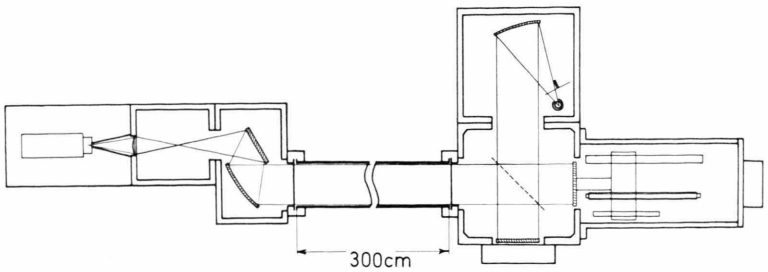

Fig. 1. Modified FS-720 interferometer with 3 m cell between beamsplitter and beamcondenser compartments.

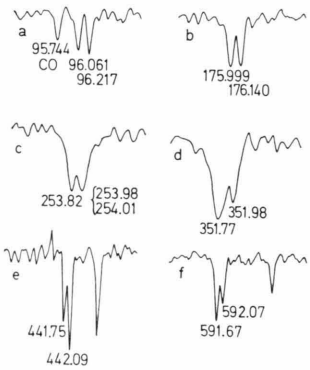

Fig. 2. Spectra of water vapour at room temperature in the 3 m cell. a, b and c are from a single, unapodized interferogram of 5150 points, sampling distance (s. d.) 16 μ, spectral window (w.) 400−50 cm^{-1}, approximately 100 mm Hg CO and <1 mm Hg H_2O. The frequencies given are from [6, 7, 18]. d, e, and f are mean values of two spectra, each from unapodized 8200 point interferograms. d: ≈4 mm Hg H_2O, s.d.= 8 μ, w. = 650−150 cm^{-1}. The frequencies given in [6] are 351.80 and 351.98 cm^{-1}. e and f: 15 mm Hg H_2O, s.d.=4 μ, w.=650−400 cm^{-1}. Note that the wavenumber scale is four times smaller than in a−d. The frequencies are from [6] and [19].

Fourier transformation, which was done on a Telefunken TR 440 computer. The Cooley-Tukey algorithm [4] was used, giving a calculating time of about 2 minutes, not including paper tape reading, plotting, etc. The interval of the spectral points was 0.038 cm^{-1}, corresponding to 16 384 calculated points. Before the computation, the phase error of the interferogram was determined by fitting a parabola to its maximum. The phase correction was made according to Loewenstein [5].

After the transformation and calculation of the mean value of two to eight spectra, the absorption maxima were determined by a polynomial fit to the curve points of each peak. The method is given in the Appendix.

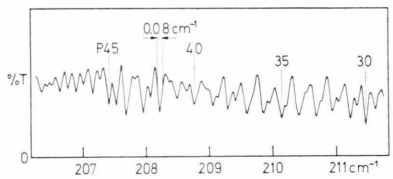

Fig. 3. Diacetylene, part of ν_9 at maximum resolution ≈0.08 cm^{-1}. Mean value of 4 spectra, each from unapodized 12000 point interferograms, s.d.=8 μ, w.=400−50 cm^{-1}, 3 m cell, ≈1 mm Hg, −70 °C.

It should be noticed that the spectra presented here contain only noise components with half widths comparable to those of the lines. Grating spectra in contrast, are normally recorded such that most of the noise peaks have much smaller half widths than the absorptions. The present noise pattern gives rise to relatively large but localized perturbations, which may lead to missing or split rotational lines. To guard against this, several independent spectra have been evaluated.

Due to the finite aperture of source and detector and to a slight error in the nominal step width, which in the FS-720 is given by a Moiré grating system, the wavenumber scale of the spectra had to be calibrated against known absorption frequencies of CO [6], H_2O [6, 7] and N_2O [8]. The frequency correction could be expressed as:

$$\nu = \nu_m + 2.2(\pm 0.2)\cdot 10^{-4}\,\nu_m\,,$$

where ν is the vacuum wavenumber and ν_m the measured wavenumber.

2. The FIR Spectrum of Diacetylene

The HC≡C−C≡CH molecule is interesting because it is the simplest hydrocarbon with two conjugated triple bonds. It has been the subject of several investigations, most recently an electron diffractio study by Tanimoto et al. [9]. As mentioned in the latter paper a discrepancy exists between the B_0-

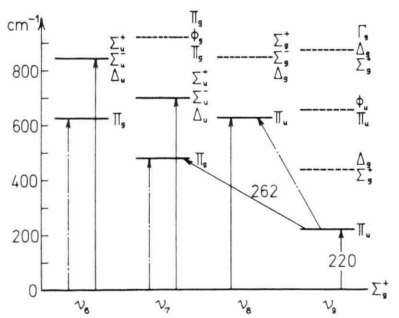

Fig. 4. Vibrational levels of Diacetylene below 900 cm^{-1} according to [14]. Calculated levels are given as dashed lines, observed infrared transitions as full, Raman transitions as broken thinner lines.

value determined from the rotational Raman spectrum [10] and from the infrared rotation vibration bands [11, 12]. Tanimoto et al. were not able to settle the question conclusively because the vibrational amplitude correction to be applied was uncertain. The far infrared spectrum of diacetylene has been measured with low resolution by Miller et al. [13], who obtained a band contour in agreement with the present spectrum shown in Figs. 5 and 6, but who did not assign $\nu_7 - \nu_9$.

The lowest energy levels of diacetylene according to [14] are illustrated in Figure 4. Near ν_9 several hot transitions are to be expected. Indeed, the band in Fig. 5 shows a series of equally spaced Q-branches of diminishing intensity. It may be assumed that these are due to
$(\nu_9 + n\,\nu_9) - n\,\nu_9$ with $n = 1, 2, 3 \ldots$ and $l' - l'' = +1$. Other transitions such as $(\nu_i + \nu_9) - \nu_i$ with $i = 6, 7, 8$ must also be considered, however. The frequencies of the Q branches of the three observed hot bands are 218.6, 217.1, and 215.7 ± 0.1 cm^{-1}.

Similarly, $\nu_7 - \nu_9$ is overlapped by other bands, of which $(\nu_7 + \nu_9) - 2\,\nu_9$ with $l = 2$ and $l = 0$ should be the two strongest. To suppress these disturbing bands, most recordings were made at a cell temperature of -70 °C. The diacetylene was prepared as described in [14] and its purity checked by comparing the known mid infrared spectra. ν_4 was found to be weaker than observed by Jones [14], but otherwise the spectra were identical.

Due to the nuclear spin statistics of this $D_{\infty h}$ molecule [15] the ν_9 band should show an intensity alternation with transitions of odd J'' three times as intense as those of even J''. In Fig. 5 this intensity pattern is seen weakly but distinctly in several parts of the band, e. g. near R(60), R(15), and P(17), leading to an unambiguous assignment, since both ν_0 and B_0 change to quite unacceptable values upon changing J by two units. Table 1 lists the assigned lines together with the deviations calculated from a least squares fit to the expression

$$\nu(m) = \nu_0 - B' - D + (B' + B'' + 2\,D)\,m + (B' - B'' + 2\,D)\,m^2 - 4\,D\,m^3 \qquad (1)$$

in which $m = -J$ for the P branch and $m = J + 1$ for the R branch transitions.

The spectra were recorded at four different pressures, and the frequencies of Table 1 are weighted means taken from the best parts of each recording. Lines with J numbers up to 100 have been observed

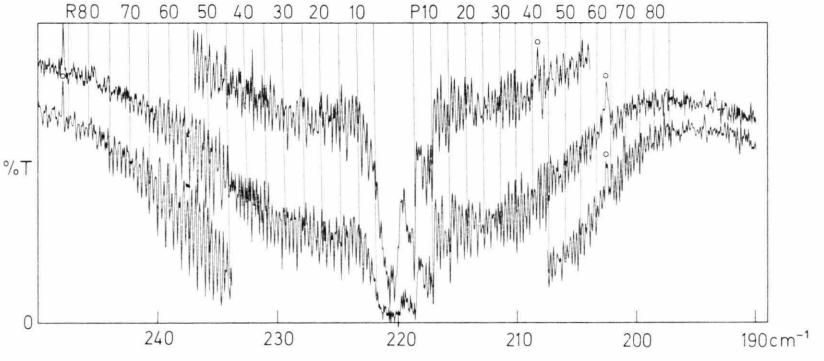

Fig. 5. ν_9 band of diacetylene, recorded at -70 °C at pressures of 10, ≈ 2 and < 1 mm Hg. The transmission scale has been shifted slightly for the highest and lowest pressure spectrum to prevent overlapping. A few negative lines due to residual water vapour in the interferometer are marked ○. The spectra are mean values of 4.8 and 4 recording s from unapodized interferograms of 8200–12500 points. s.d. = 8 μ, w. = 400–50 (or 150) cm^{-1}, resolution ≈ 0.12 cm^{-1}.

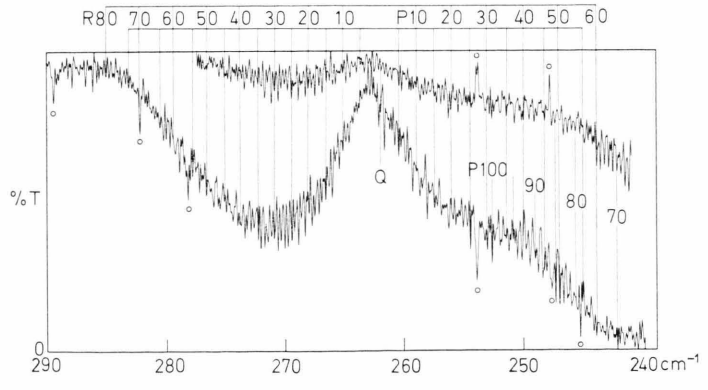

Fig. 6. $\nu_7 - \nu_9$ band of diacetylene, recorded at +25 °C, 80 mm Hg and -70 °C, 10 mm Hg (continuation of spectrum of Figure 4). The lines P 100–70 are from the ν_9 band. H_2O lines are marked ○. The spectra are mean values of 2 and 4 Fourier transforms of 8200 point unapodized interferograms. s.d. = 8 μ, w. = 400–50 cm^{-1}, resolution ≈ 0.1 cm^{-1}.

Table 1. Line frequencies of the ν_9 band of diacetylene. δ is the difference between the observed line frequencies and those calculated from Eq. (1) with the constants of Table 2.

J	$R(J)$ cm^{-1}	100 δ cm^{-1}	$P(J)$ cm^{-1}	100 δ cm^{-1}	J	$R(J)$ cm^{-1}	100 δ cm^{-1}	$P(J)$ cm^{-1}	100 δ cm^{-1}
5	221.790	2.7	218.535	.2	54	237.060	.4		
6	222.059	−.2	218.241	−.3	55	237.394	1.1	204.807	−1.5
7	222.366	.7	217.918	−3.7	56	237.710	−.1	204.575	1.1
8	222.659	.2			57	238.047	.8	204.292	−1.5
9	222.965	.9	217.364	−1.4	58	238.375	.7	204.028	−2.2
10	223.255	−.1	217.119	2.8	59	238.712	1.3	203.792	−.3
11	223.556	−.0	216.788	−1.6	60	239.036	.7	203.515	−2.5
12	223.857	−.0	216.509	−.9	61	239.368	.8		
13	224.174	1.5	216.223	−1.0	62	239.681	−1.0	203.029	−.2
14	224.464	.3	215.944	−.3	63	240.038	1.5	202.766	−1.2
15	224.780	1.6	215.673	1.0	64	240.383	2.7		
16	225.075	.6	215.383	.3	65	240.721	3.2	202.264	−.9
17	225.380	.7	215.089	−.8	66	241.019	−.4	202.028	.6
18	225.685	.8	214.795	−2.0	67	241.363	.6	201.773	.2
19	226.006	2.3	214.512	−2.1	68	241.673	−1.9	201.506	−1.5
20			214.242	−1.0	69	242.027	−.0	201.285	1.3
21	226.605	1.0	213.964	−.8	70	242.353	−1.1	200.995	−2.9
22					71	242.691	−.9	200.770	−.6
23	227.211	.1	213.402	−1.1	72	243.033	−.5	200.537	.9
24	227.475	−4.4	213.117	−1.8	73	243.377	.1	200.285	.3
25	227.799	−2.9	212.850	−.7	74	243.724	.9	200.034	−.2
26	228.112	−2.5	212.587	.7	75	244.054	.0	199.804	1.3
27	228.450	.2	212.297	−.6	76	244.394	.0	199.557	1.1
28	228.764	.6			77	244.734	.0	199.307	.5
29	229.084	1.4	211.763	1.1	78	245.054	−2.1	199.054	−.5
30	229.390	.8			79	245.404	−1.2	198.809	−.8
31	229.700	.4	211.212	.9	80	245.784	2.6	198.591	1.6
32	230.035	2.6	210.932	.2	81	246.114	1.3	198.332	−.1
33	230.333	1.0	210.675	1.8	82	246.464	2.0	198.114	2.1
34	230.638	.1	210.404	1.9	83	246.785	−.3	197.844	−.9
35	230.947	−.6	210.133	1.9	84	247.104	−2.8	197.633	2.0
36	231.264	−.4	209.854	1.1	85	247.454	−2.3	197.373	−.1
37	231.580	−.5	209.599	2.6	86			197.163	2.7
38	231.901	−.1	209.319	1.5	87	248.175	.6	196.943	4.4
39	232.221	.2	209.061	2.6	88	248.505	−1.1	196.673	1.1
40	232.549	1.2	208.771	.4	89	248.885	2.2	196.393	−3.3
41	232.847	−.9	208.500	.1	90			196.163	−2.8
42	233.178	.3	208.229	−.3	91	249.575	1.6	195.963	.6
43	233.491	−.4	207.966	−.0	92	249.875	−3.3	195.713	−1.0
44	233.828	1.2	207.714	1.3	93	250.235	−2.3	195.503	1.3
45	234.117	−2.0	207.428	−.8	94	250.605	−.3	195.253	−.4
46	234.461	.1	207.173	.2	95	250.955	−.4		
47			206.913	.5	96	251.315	.5		
48	235.090	−1.5	206.645	.1	97	251.655	−.7	194.573	1.0
49	235.397	−3.2	206.371	−1.1	98	252.035	2.0		
50	235.735	−1.8	206.111	−.9	99			194.073	−3.1
51	236.058	−2.0	205.840	−1.9	100				
52	236.398	−.5			101	253.096	2.0		
53	236.729	−.0							

at room temperature and a pressure of 80 mm Hg, for the first time allowing a determination of the very small D constant. The weaker hot transitions are not listed in Table 1, because most of them are blends. Some obviously blended lines of the main band have been omitted in the calculation of the rotational constants given in Table 2. B_0 compares well with the previous infrared values of 0.1464_1 [11] and 0.1463_8 cm^{-1} (see [12]) (both $\pm 10^{-4}$ cm^{-1}).

The assignment of the $\nu_7 - \nu_9$ band (Fig. 6) presented some difficulty, mostly because of the heavily overlapped B-branch and the absence of an easily destinguishable Q-branch. The following procedure was adopted: From the ν_9-analysis B_{9c}, the rotational constant of the lower component of the Π_u level, was known [B' of Equation (1)]. By applying the empirical relation [16]

$$q_i \approx 2.6\, B_0^2/\nu_i \qquad (2)$$

a preliminary value of B_{9d}, the rotational constant of the upper component of the Π_u level, could be calculated, and by means of a graphical plot [17] (Loomis-Wood plot) the assignment was established. Because of the interfering hot bands and the rather low signal-to-noise ratio only the lines with high statistical weight (3 : 1) could be identified. It is seen from Fig. 7 that one set of lines (with J''

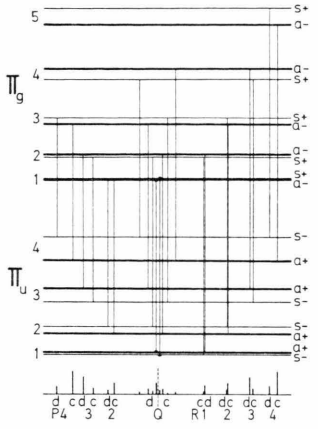

Fig. 7. Energy level diagram for a $\Pi_g \leftarrow \Pi_u$ band of diacetylene. The l-type doubling is exaggerated, and it has been assumed that $B'=B''$ and $2q' \approx q''$. It is seen that the P and R branch transitions between levels of (nuclear spin) statistical weight 3 form two series: One, connecting the lower (c) levels of even J'', and one connecting the d levels.

even) could be used for determining the rotational constants of the c component and one set (J'' odd) for the d component of the band. It should be noticed that the observed c and d frequency sets are not quite independent. The line systems cross each other, leading to a periodic enhancement of the transitions, where they happen to coincide. The frequencies of such regions have been used for the rotational analysis of both the c and d components.

Within the experimental accuracy, the analysis of the $\nu_7-\nu_9$ band must yield the same value of B_{9c} as was obtained from the ν_9 fundamental. Thus the assignment of the $\nu_7-\nu_9$ band could be checked by changing the J numbering by ± 2 units. The B_{9c} value for $J_1=J+2$ was also acceptable, but the present assignment is preferred, because in this case a small Q branch could be identified. Furthermore, ν_0 is nearer the pronounced band minimum with the assignment of Table 3. The assigned J values for $\nu_7-\nu_9$ do not extend as high as for the ν_9 band, and the line frequencies scattered more, so that no D constant could be determined. The expression

Table 2. Vibrational frequencies and rotational constants for diacetylene. (The figures given in parentheses are three times the standard error, in units of the last significant figure. A calibration error of $\pm 5\times10^{-3}$ cm^{-1} is not included in the quoted precision of ν_9 and ν_7.)

1. Constants, obtained directly: (cm^{-1})

ν_9	$(\nu_7-\nu_9)$ c	$(\nu_7-\nu_9)$ d
$\nu_0=$ 220.139 (5)	$\nu_0=$ 261.99 (1)	$\nu_0=$ 261.99 (1)
$B''=B_0=$ 0.14649 (7)	$B''=B_{9c}=$ 0.1467 (2)	$B''=B_{9d}=$ 0.1474 (2)
$B'=B_{9c}=$ 0.14680 (7)	$B'=B_{7c}=$ 0.1466 (2)	$B'=B_{7d}=$ 0.1472 (2)
$B'-B''=$ $3.13(1)\times10^{-4}$	$B'-B''=$ $-0.92(7)\times10^{-4}$	$B'-B''=$ $-1.93(6)\times10^{-4}$
$D=$ $2.1(6)\times10^{-8}$		

2. Derived constants: (cm^{-1})

$\nu_7=(\nu_7-\nu_9)+\nu_9=482.13(1)$
$B_{7c}=B_{9c}+(B_{7c}-B_{9c})=0.14671(7)$
$B_{7c}-B_0=(B_{7c}-B_{9c})+(B_{9c}-B_0)=2.21(7)\times10^{-4}$
$q_7-q_9=(B_{7d}-B_{9d})-(B_{7c}-B_{9c})=-1.02(9)\times10^{-4}$

used for the least squares fit to each component of $\nu_7-\nu_9$ (for which $l'=l''=1$) was

$$\nu(m)=\nu_0-B'+B''+(B'+B'')\,m+(B'-B'')\,m^2. \tag{3}$$

Table 3 lists the assigned lines of $\nu_7-\nu_9$ together with the differences between observed and calculated line positions. Some of the line frequencies of high J transitions of the R branch of ν_0 with even J'' were also used in the analysis of $\nu_7-\nu_9$, because much of the line intensity is believed to originate in $\nu_7-\nu_9$ transitions. These frequencies are thus listed both in Table 1 and in Table 3.

The vibrational frequency $\nu_7-\nu_9$ as obtained from the c and d band components agrees within 0.004 cm^{-1} and coincide closely with the frequency 262 cm^{-1} calculated from the low resolution Raman measurement of ν_7(gas) [14].

A reliable determination of the l-type doubling constants q_7 and q_9 was not possible because of the low accuracy of B_{7d} and B_{9d}, but

$$q_7-q_9=(B_{7d}-B_{9d})-(B_{7c}-B_{9c})$$

agrees well with the theoretical estimate from Eq. (2) of 1.4×10^{-4} cm^{-1} (see Table 2). A more accurate value of B_{7c} than that obtained directly from the least squares fit to Eq. (3) was calculated from $B_{7c}=B_{9c}+(B_{7c}-B_{9c})$, utilizing B_{9c} from the ν_9 fundamental and $(B_{7c}-B_{9c})$ from $\nu_7-\nu_9$.

Table 3. Line frequencies of the $\nu_7-\nu_9$ band of diacetylene. δ is the difference between the observed line frequencies and those calculated from Eq. (3) with the constants of Table 2.

	c component					*d* component			
J	*R*(*J*) cm^{-1}	100 δ cm^{-1}	*P*(*J*) cm^{-1}	100 δ cm^{-1}	*J*	*R*(*J*) cm^{-1}	100 δ cm^{-1}	*P*(*J*) cm^{-1}	100 δ cm^{-1}
4			260.814	−.3	5			260.482	−2.9
6	264.043	.3	260.246	1.7	7	264.333	−.0	259.889	−2.8
8	264.630	.6	259.630	−1.0	9	264.943	2.7	259.292	−2.9
10	265.202	−.5	259.017	−3.3	11	265.496	−.0	258.695	−3.0
12	265.816	2.7			13	266.073	−.3	258.135	.9
14	266.338	−3.3	257.854	−1.4	15	266.626	−2.8		
16	266.970	1.8	257.240	−3.6	17	267.225	−.5	256.929	.4
18	267.567	3.5	256.667	−1.6	19	267.828	2.4	256.306	−1.5
20	268.137	2.6			21	268.375	−.2	255.699	−1.7
22	268.677	−1.2	255.507	1.2	23	268.953	.5	255.091	−1.9
24	269.308	4.1	254.882	−1.8	25	269.520	.2	254.485	−1.7
26	269.852	.8	254.311	.6	27	270.109	2.3		
28	270.416	−.4			29	270.663	.9	253.285	.3
30	270.980	−1.6	253.093	−1.8	31	271.233	1.4	252.705	3.5
32	271.541	−3.0	252.482	−3.1	33	271.804	2.1	252.031	−2.4
34	272.140	−.5	251.915	.1	35	272.361	1.6		
36	272.708	−1.1	251.310	−.5	37	272.933	2.8	250.818	−.4
38	273.292	.1			39	273.499	3.5		
40			250.097	−1.7	41			249.571	−1.3
42	274.430	−.4			43			248.930	−3.2
44			248.930	2.0	45			248.350	1.1
46	275.570	−.5	248.350	4.3	47			247.750	3.7
48	276.134	−1.0	247.750	4.8	49			247.105	1.8
50	276.722	1.0	247.105	.7	51	277.309	−2.6	246.468	.9
52	277.309	3.0	246.468	−2.5	53	277.897	1.6		
54	277.897	5.1			55	278.419	−.7	245.225	2.6
56	278.419	.7			57	278.973	.3		
58	278.973	−.4			59				
60					61				
62	280.080	−2.6			63	280.610	1.8		
64					65				
66					67	281.648	−1.7		
68					69				
70					71				
72	282.942	2.8			73	283.223	−4.0		
74	283.467	−.7			75	283.795	.2		
76	284.013	−1.9			77				
78					79	284.845	−.3		
80					81	285.368	−.5		
82	285.677	−2.8			83				

Appendix

The line maxima were determined by a program using the following procedure:

The points between two successive absorption minima are isolated, and to eliminate most of the noise only lines with a maximum of $k\%$ absorption relative to at least one minimum are accepted. k has generally been given a value bteween 5 and 10. The degree n of the polynomial is determined from the highest number of points $(n+1)$ available symmetrically on both sides of the maximum upon including the nearest minimum. n is limited to a pre-set value, in this work 7.

The polynomial is now calculated and its maximal value sought by interpolation in steps of one tenth of the original point distance, here 0.038 cm^{-1}. The program has been tested by manual evaluation of a number of lines. The agreement was always better than 0.01 cm^{-1} for a point distance as above.

Acknowledgements

The numerical calculations were carried out at the computer centers of the universities of Kiel and Hamburg. The original version of the Fourier transform program was kindly provided by Dr. C. Irslinger, Stuttgart. Dr. B. P. Winnewisser is thanked for several helpful discussions and the Deutsche Forschungsgemeinschaft for financial support.

[1] T. Stroyer-Hansen, Infrared Phys. **10**, 159 [1970].
[2] L. W. Thorpe, D. J. Neale, and G. C. Hayward, Aspen Internat. Conf. Fourier Spectry., 1970, p. 187 (AFCRL-71-0019).
[3] R. J. Bell, Introductory Fourier Transform Spectroscopy, Academic Press, New York 1972, p. 63 ff.
[4] J. W. Cooley and J. W. Tukey, Math. Comput. **19**, 297 [1965].
[5] E. V. Loewenstein, Appl. Opt. **2**, 491 [1953].
[6] K. Narahari Rao, C. J. Humphreys, and D. H. Rank, Wavelength Standards in the Infrared, Academic Press, New York 1966.
[7] R. T. Hall and J. M. Dowling, J. Chem. Phys. **52**, 1161 [1970].
[8] I. U. P. A. C. Tables of Wavenumbers for Calibration of Infra-Red spectrometers, Butterworths, London 1961.
[9] M. Tanimoto, K. Kuchitsu, and Y. Morino, Bull. Chem. Soc. Japan **44**, 386 [1971].
[10] J. H. Callomon and B. P. Stoicheff, Can. J. Phys. **35**, 373 [1957].
[11] A. Vallance Jones, J. Chem. Phys. **20**, 860 [1952].
[12] G. D. Craine and H. W. Thompson, Trans. Faraday Soc. **49**, 1273 [1953].
[13] F. A. Miller, D. H. Lemmon, and R. E. Witkowski, Spectrochim. Acta **21**, 1709 [1965].
[14] A. Vallance Jones, Proc. Roy. Soc. London **A 211**, 285 [1952].
[15] G. Herzberg, Infrared and Raman Spectra of Polyatomic Molecules, Van Nostrand, New York 1945, p. 16.
[16] C. H. Townes and A. L. Schawlow, Microwave Spectroscopy, McGraw-Hill, London 1955, p. 33.
[17] F. W. Loomis and R. W. Wood, Phys. Rev. **32**, 223 [1928]. J. F. Scott and K. Narahari Rao, J. Mol. Spectr. **20**, 461 [1966].
[18] R. T. Hall and J. M. Dowling, J. Chem. Phys. **47**, 2454 [1967].
[19] J. R. Izatt, H. Sakai, and W. S. Benedict, J. Opt. Soc. Am. **59**, 19 [1969].

Der Jahn-Teller-Effekt des Cu^{2+}-Ions in tetraedrischer Sauerstoffkoordination

I. Ligandenfeldspektroskopische Untersuchungen an Cu^{2+}-haltigen oxidischen Gittern

D. Reinen und J. Grefer

Fachbereich Chemie der Universität Marburg

(Z. Naturforsch. **28 a**, 1185—1192 [1973]; eingegangen am 29. März 1973)

Ligand field spectra of Jahn-Teller-distorted CuO_4-tetrahedra in oxidic solids

The ligand field reflectance spectra of tetrahedrally coordinated Cu^{2+}-ions in different oxidic host structures (several spinel compounds, $Ca_2ZnSi_2O_7$, Zn_2SiO_4, several garnets, ZnO) and at different temperatures (300 °K—4 °K) are analysed. For Cu^{2+}-ions in compressed tetrahedra with D_{2d}-symmetry the two expected bands: $^2B_2(^2T_2) \rightarrow {}^2E(^2T_2)$ $[t_1]$ and $^2A_1(^2E)$ $[t_3]$ respectively were found, while in cases of lower symmetry the transition $^2B_3(^2T_2) \rightarrow {}^2B_1(^2E)$ $[t_2]$ is observed in addition. For the spinel mixed crystal series $[Zn_{1-x}Cu_x]^{(4)}[Cr_2]^{(6)}O_4$ $(0 \leqq x \leqq 1{,}0)$ a first order transition from the cubic to a tetragonal $(c/a < 1)$ structure occurs at $x = 0.47$. The transitions t_1 and t_3 show a remarkable UV-shift for $x > 0{,}47$, indicating an increasing Jahn-Teller distortion of the CuO_4-tetrahedra with increasing x. The Jahn-Teller-splitting of the $^2T_2$-groundstate $[t_1]$ was found to range between $\approx 3000\ cm^{-1}$ and $8500\ cm^{-1}$ for the different compounds. The bands could be fitted using "angular overlap" parameters e_λ $(\lambda = \sigma, \pi_\perp, \pi_\parallel)$. Finally the spectrum of Cu^{2+}-doped ZnO could be analysed on the basis of trigonally compressed CuO_4-tetrahedra with a $^2T_2$-ground-state splitting of $\approx 3000\ cm^{-1}$.

I. Einleitung

In mehreren vorangegangenen Veröffentlichungen (l. c. [1–6]) haben wir uns eingehender mit den spektroskopischen und strukturellen Konsequenzen der Jahn-Teller-Instabilität des ^2E_g-Grundterms des Cu^{2+}-Ions in vorgegebenen oktaedrischen Umgebungen von Sauerstoff und Stickstoff beschäftigt. In dieser Arbeit möchten wir die Ergebnisse einiger systematischer Untersuchungen am Cu^{2+}-Ion in tetraedrischer Sauerstoffumgebung diskutieren, da über die spektroskopischen und strukturellen Aspekte eines Jahn-Teller-instabilen T_2-Terms bisher nur wenige experimentelle Daten vorliegen.

Das Cu^{2+}-Ion in tetraedrischer Umgebung besitzt einen bahnentarteten T_2-Grundzustand $(e^4 t_2^5)$, der im einfachsten Fall durch eine *tetragonale Stauchung* entlang einer S_4-Achse oder eine *trigonale Stauchung* entlang einer dreizählige Achse so aufgespalten werden kann, daß — dem Jahn-Teller-Theorem entsprechend — ein neuer *einfacher* Grundzustand resultiert (Abbildung 1). Von den drei möglichen Übergängen in D_{2d} ist derjenige nach B_1 symmetrieverboten, während für die C_{3v}-Symmetrie beide möglichen Übergänge im Ligandenfeldspektrum zu beobachten sein

Sonderdruckanforderungen an Prof. Dr. D. Reinen, Fachbereich Chemie der Philipps-Universität Marburg/Lahn, *D-3550 Marburg*/Lahn, Lahnberge.